Diamond & Related Materials 136 (2023) 109912

Contents lists available at ScienceDirect

Diamond & Related Materials

journal homepage: www.elsevier.com/locate/diamond

Quasi-isotropic high pressure, large volume synthesis of a polymeric composite incorporating diamond-like carbon nano-threads

Samuele Fanetti [a,b,*], Sebastiano Romi [b,g], Wilson Crichton [c], Anja Rosenthal [c,d], Demetrio Scelta [a,b], Frederico Alabarse [e], Roberto Bini [f,a,b], Mario Santoro [g,b,**]

[a] Consiglio Nazionale delle Ricerche - Istituto di Chimica dei Composti OrganoMetallici, Via Madonna del Piano 10, Sesto Fiorentino 50019, FI, Italy
[b] European Laboratory for Nonlinear Spectroscopy (LENS), Via Nello Carrara 1, Sesto Fiorentino 50019, FI, Italy
[c] European Synchrotron Radiation Facility, ESRF, 71 Avenue des Martyrs, Grenoble, CS40220, Cedex 9, France
[d] Research School of Earth Sciences, The Australian National University, Canberra, ACT 2601, Australia
[e] Elettra Sincrotrone Trieste S.C.p.A, AREA Science Park, Basovizza 34149, TS, Italy
[f] Dipartimento di Chimica "Ugo Schiff", Università di Firenze, via della Lastruccia 3, Sesto Fiorentino 50019, FI, Italy
[g] Consiglio Nazionale delle Ricerche - Istituto Nazionale di Ottica, Via Nello Carrara 1, Sesto Fiorentino 50019, FI, Italy

ARTICLE INFO

Keywords:
Hydrogenated, diamond-like carbon nano-threads
High pressure synthesis
Multianvil large-volume press
Synchrotron X-ray diffraction
Optical spectroscopy

ABSTRACT

The high pressure synthesis of hydrogenated, sp^3-hybridized carbon nanothreads from aromatics is a vibrant research area. These nanomaterials are expected to join the high tensile strength of diamond with the high flexibility of polymers. The smart selection of the initial aromatic substance leads to tailor transport and optical properties and to enhance the selectivity of the synthesis. So far, the synthesis has only been performed in two-opposed anvils cells, supporting large uniaxial stress. To increase chemical selectivity and yield, the interplay between this stress and the intrinsic relative molecular orientation in the starting crystal is a very important aspect to clarify. We report the synthesis (30 GPa) of a diphenylacetylene-derived polymeric composite incorporating domains of potentially semiconductive C-nanothreads, performed in a large volume, multi-anvil two-stage press. This device provides quasi-isotropic direct compression of millimeter-sized samples. Materials characterizations were performed by synchrotron, powder X-ray diffraction and Infrared spectroscopy. The product is quite similar to those previously obtained in diamond anvil cells, showing that the synthesis is not related to uniaxial stress and is instead driven by the favourable intermolecular orientation in the initial molecular solid. These findings are very likely to be common to many other aromatic systems, and also show the scalability to large volumes of the C-nanothreads synthesis.

1. Introduction

Hydrogenated, sp^3-hybridized C-nanothreads, one among several known extended hydrocarbon compounds, were first discovered upon room temperature compressions of the aromatic archetype, benzene, slightly above 20 GPa [1–3]. Indeed, chemical reconstruction led to form overall linear, diamond-like structures with transverse shape and size reflecting those of the starting monomer. These unique materials are expected to combine the high tensile strength of diamond to the high flexibility of polymers. Benzene-derived C-nanothreads pack together with no long range order along the thread axis and 2D close packed, pseudo-hexagonal crystalline order in the orthogonal plane. More recently, carbon nanothreads bearing a sort of azimuthal order around the thread axis and even long-range order along the axis were synthesized at high pressures from thiophene [4], and triazine [5] and pyridazine [6], respectively. Along with these cases, many other types of C-nanothreads were synthesized at high pressures starting from a number of polycyclic, hetero- and substituted aromatic compounds [7–17]. As a consequence, the current understanding is that the high pressure transformation of simple aromatic systems into nanothreads is a quite general property for these substances. On the other hand, the purpose of operating a smart selection of the initial aromatic substance is at least

* Correspondence to: S. Fanetti, Consiglio Nazionale delle Ricerche - Istituto di Chimica dei Composti OrganoMetallici, Via Madonna del Piano 10, Sesto Fiorentino 50019, FI, Italy.
** Correspondence to: M. Santoro, Consiglio Nazionale delle Ricerche - Istituto Nazionale di Ottica, Via Nello Carrara 1, Sesto Fiorentino 50019, FI, Italy.
E-mail addresses: fanetti@lens.unifi.it (S. Fanetti), santoro@lens.unifi.it (M. Santoro).

https://doi.org/10.1016/j.diamond.2023.109912
Received 17 January 2023; Received in revised form 31 March 2023; Accepted 3 April 2023
Available online 7 April 2023

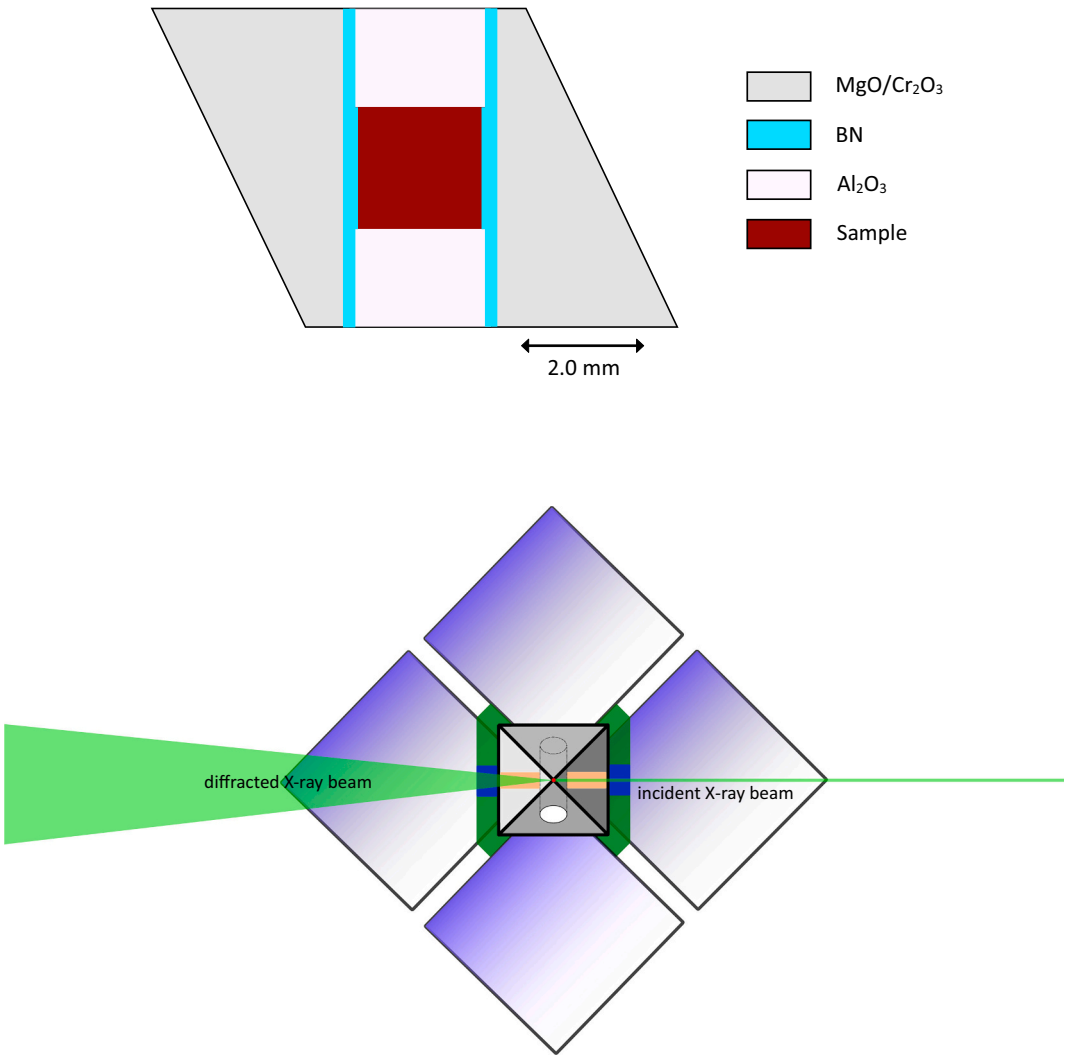

Fig. 1. Second-LVP-stage/sample configuration. Top: cross section of the octahedral assembly with materials description. Bottom: positioning of the octahedral assembly between the WC cubes. Yellowish cylinders through the assembly: SiBCN X-ray windows. Blue section through the green gasket: MgO. (For interpretation of the references to colour in this figure legend, the reader is referred to the web version of this article.)

twofold. From one side, this choice is aimed to add useful physical properties to nanothreads such as transport and optical properties, without worsening their unique mechanical features. In addition, a proper selection of the starting molecular system can lead to enhance the selectivity of the chemical synthesis of internally ordered or quasi-ordered C-nanothreads with respect to unwanted side products. Yet, to increase selectivity and yield, it is very important to investigate, on a general ground, the interplay between the anisotropy of the applied loads usually affecting the synthesis protocols, and the nature of the intermolecular interactions at work in the starting molecular crystal, a point of still intense debate. This debate is currently limited to syntheses performed via two opposed anvil cells such as diamond anvil cells (DACs) and Paris-Edinburgh (PE) cells with no pressure transmitting medium (PTM), with only two exceptions: sp^3 C-nanothreads synthesized from aromatic $C_{10}H_8C_{10}F_8$ co-crystals in DACs, with Ne or He as the PTM [18,19]. In the case of C-nanothreads obtained in DACs and PE with no PTM, the formation of the products occurred in the presence of strong uniaxial stress. For benzene-derived nanothreads, the uniaxial stress was shown to be the driving force of the synthesis and, consequently, the chemical reaction to be non-topochemical [1–3], whereas topochemical or nearly topochemical pathways led to C-nanothreads starting from several lower symmetry aromatics such as aniline [11,12], triazine [5], azobenzene [16], and disubstituted benzene [14]. In the topochemical reactions, the favourable, nearest neighbours intermolecular orientation plaid the major role in driving the transformations and the extended product nearly and selectively reflected the topology of the molecular precursor. In order to deepen our understanding on the interplay between different potential reaction mechanisms in the nanothreads synthesis, it would be more than natural to conceive high pressure syntheses where the uniaxial load scheme of DACs and PE is modified and, possibly, the uniaxial stress removed. The results should then be compared to those obtained by using two-opposed anvil cells. This is precisely one of the two main purposes of the present work. We accomplished this task by using a multi-anvil large volume press (MALVP) exploiting an octahedral geometrical scheme for the applied loads, hence a quasi-isotropic one as compared to DACs and PE. As the case system, we focused on diphenylacetylene (DPhA). In fact, we have recently synthesized DPhA-derived polymeric composites incorporating carbon nanothreads using DACs [20], so we do have solid reference DAC results to compare with the MALVP data. In addition, these nanothreads are an interesting, unique semiconductive version of C-nanothreads actually made of double core diamond-like nanothreads with the two cores being bound by a conjugated C, polyacetylene-like backbone. This material exhibits an optical bandgap of 1.74 eV, similar to

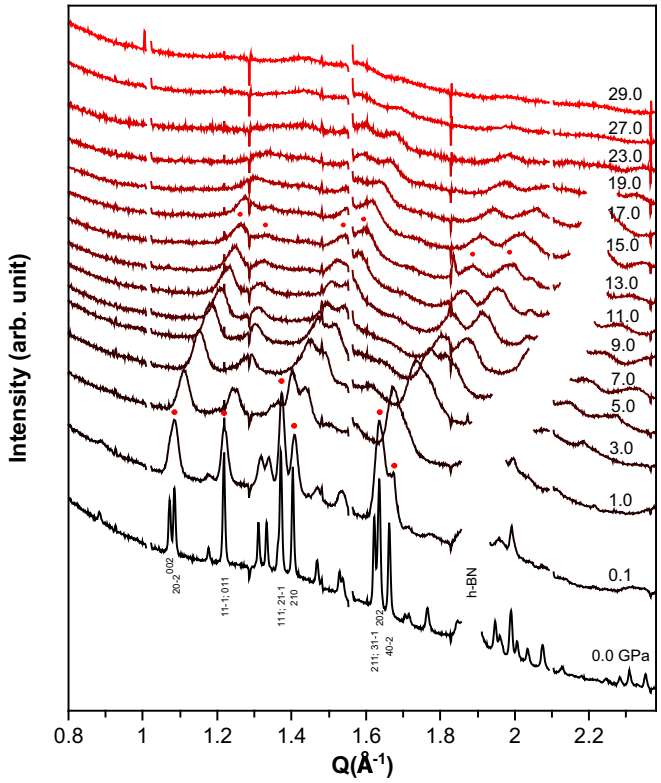

Fig. 2. selected powder XRD patterns (λ = 0.389887 Å) of DPhA measured upon increasing pressure, from bottom to top. All peaks belong to the initial molecular DPhA crystal. Vertical numeric strings: Miller indices for the strongest Bragg peaks. Red dots: marks for peaks which where used for evaluating the compression curve. The (002) peak for h-BN has been cut out and the patterns where vertically split for the sake of clarity. The large diffuse background is dominated by the Compton scattering from the long (~2 m) air path between the sample and the detector. Glitches come from the gaps between the detector chips. (For interpretation of the references to colour in this figure legend, the reader is referred to the web version of this article.)

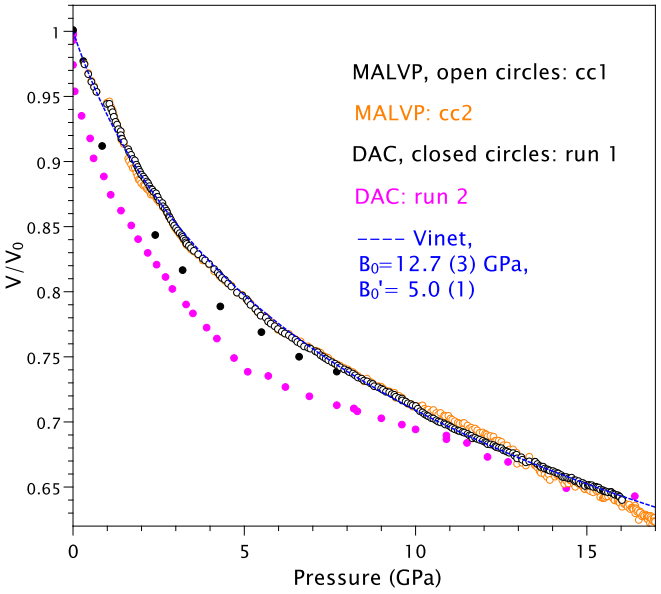

Fig. 3. Compression curves of the molecular diphenylacetylene crystal. Black and orange open circles: MALVP data from the same run, processed through two distinct procedures called cc1 and cc2, respectively (see text). Full black and magenta circles: DAC data for two different samples obtained in an experiment described previously [20]. Blue, dashed line: Vinet equation of state fitted to the cc1 MALVP compression curve. (For interpretation of the references to colour in this figure legend, the reader is referred to the web version of this article.)

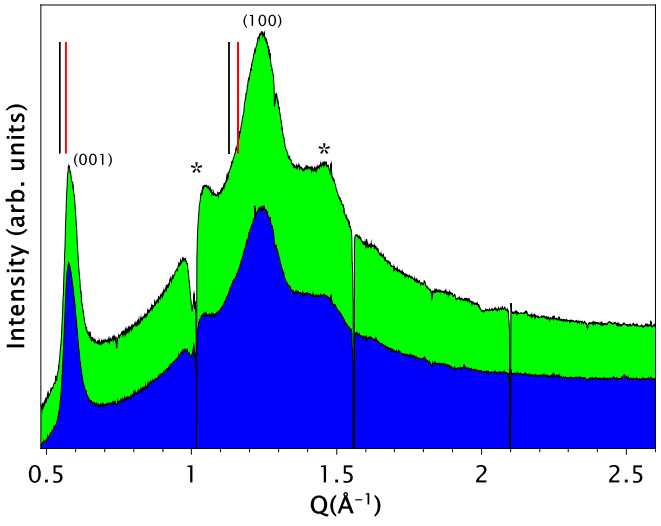

Fig. 4. Ex-situ XRD patterns (λ = 0.389887 Å) of the post synthesis (MALVP) recovered sample, measured at two distinct points (green and blue). A background diffuse scattering signal, mostly due to the Compton scattering of air, has been subtracted and the patterns have been vertically shifted for the sake of clarity. The two Bragg peaks labelled by Miller indices are assigned to 2D packed, double-core C-nanotheads derived from DPhA (see text). Vertical, black sticks: Q position for the (001) and (100) peaks observed after the sample has been relaxing for about two weeks, using a table-top XRD set-up (Mo source). Vertical, red sticks: (001) and (100) peaks observed for DPhA-derived C-nanothreads synthesized in DACs. Asterisks: Bragg peaks from the supporting tape. Glitches: gaps between the detector chips. (For interpretation of the references to colour in this figure legend, the reader is referred to the web version of this article.)

polyacetylene; it is then very attractive as a potential organic semiconductor with simultaneous outstanding mechanical properties.

The second purpose of our quest through the MALVP set-up was to scale up the synthesis of C-nanothreads as much as possible, and indeed we obtained millimiter-size volumes for the product, after compression of DPhA to 30 GPa, at room temperature. Volume scale-up has obvious potentials for technological applications of these novel materials.

In the following, we present a brief description of the experimental procedures, in situ synchrotron powder X-ray diffraction (XRD) investigations of DPhA under pressure, ex-situ XRD and Infrared (IR) spectroscopy measurements of the recovered product, and comparisons to the results obtained in DACs. The comparison shows that the two high pressure synthesis techniques led substantially to the same composite materials, incorporating the same nanothread domains, although the schemes of the applied loads differ significantly. This in turn clearly suggests that the intrinsic nearest neighbours intermolecular orientation in the molecular solid precursor is indeed favourable for the formation of nanothreads (topochemical reaction) and that this orientation, rather than the anisotropy of applied loads, provides a major contribution to those driving the synthesis.

2. Experimental methods

High pressure powder XRD measurements on crystalline diphenylacetylene (Sigma-Aldrich, purity >98 %) were performed up to 30 GPa, at

Table 1
Q position and corresponding d values for the two Bragg peaks observed in Fig. 4 for the nanothread sample synthesized in the MALVP set-up, and indexed as in our previous study in DACs [20]. The Q and d values for the same sample observed after about two weeks, MALVP relax, through our in-house diffractometer (Mo micro-source, λ = 0.71073 Å), and for samples obtained in DACs are also reported.

Sample	Q_{001} (Å^{-1})	Q_{100} (Å^{-1})	d_{001} (Å)	d_{100} (Å)	d_{001}/d_{100}
MALVP	0.5835 (3)	1.233 (3)	10.768 (6)	5.10 (1)	2.111 (4)
MALVP, relaxed	0.5489 (6)	1.129 (2)	11.44 (1)	5.56 (1)	2.056 (3)
DACs [20]	0.566 (7)	1.16 (1)	11.1 (1)	5.41 (5)	2.05 (4)

room temperature, in a large volume press (LVP) set-up at the ID06-LVP beam line of the ESRF. This device consists of a Kawai-type, two-stage multianvil apparatus driven by a 2000 ton press, with independent control on upper and lower rams to ensure triaxial compression at all loads. We used the standard 6/8 high pressure assembly with WC cubes (6UF, Sandvik) having 3 mm truncations and enclosing a 7 mm edge Cr_2O_3-doped MgO octahedron, working as the pressure transmitting medium, which in turn hosted the cylindrically shaped BN sample capsule and the sample itself (Fig. 1). We then plugged two Al_2O_3 pellets at the top and the bottom of the cylindrical sample, respectively. Pyrophyllite was used as the gasket material, with SiBCN and MgO windows along the beam path. The initial sample volume was equal to 3.1 mm^3. The sample was compressed with a pressure slope of about 0.04 GPa/min and a maximum load larger than 1000 tons, and continuous, in situ data collection of XRD patterns (1 s of collection time) was performed in order to characterize the degree of conversion. The total compression time for achieving the maximum pressure of 30 GPa was equal to about 12.5 h. Similar pressure slope and total time were adopted to decompress the sample down to ambient conditions, after having held it at the maximum pressure for about 10 h. These times are similar or in the same order of magnitude as those adopted for the synthesis of DPhA-derived carbon nanothreads in DACs. The sample pressure was measured by the BN equation of state [21,22]. XRD patterns on the ambient pressure recovered materials were also measured. The X-ray beam coupled to the LVP had an incident spot size of about 1 mm^2, when not limited by the anvil gaps, and wavelengths equal to 0.389887 Å and 0.233933 Å and we used a Pilatus3 X CdTe 900K-W (Dectris) X-ray detector. The diffractometer was calibrated using a LaB_6 powder standard, and the diffraction patterns were analyzed and integrated using FIT2D [23]. Additional X-ray data presented through the paper and measured for samples in diamond anvil cells were measured at the XPRESS beam line (λ = 0.49499 Å) of the Elettra synchrotron, by procedures described previously [20]. Fourier transform infrared (IR) absorption spectra in the medium IR frequency range were measured using a Bruker-IFS 120 HR spectrometer equipped with blackbody broadband sources and suitably modified for experiments in DACs, with a frequency resolution set to 1 cm^{-1} [24].

3. Results and discussion

In Fig. 2, we report selected XRD patterns of DPhA measured in situ in the MALVP upon increasing pressure up to 29 GPa with the maximum pressure in this run being equal to 30 GPa. In fact, this is the maximum pressure at which we previously pursued the synthesis of DPhA-derived carbon nanothreads in DACs [20]. In the figure, we have limited the Q interval to include only the strongest Bragg peaks of the molecular DPhA crystal. We observe a general positive pressure shift of the XRD patterns, and also a sudden increase in the width of all peaks between ambient pressure and about 1 GPa, while the increase is much more gradual at higher pressures. Interestingly, the peak width values observed at high pressures, which we very reasonably assign to the deviatoric stress in the sample grains and to pressure gradients here in play, are very close to those found for measurements in DACs [20]. On the other hand, the

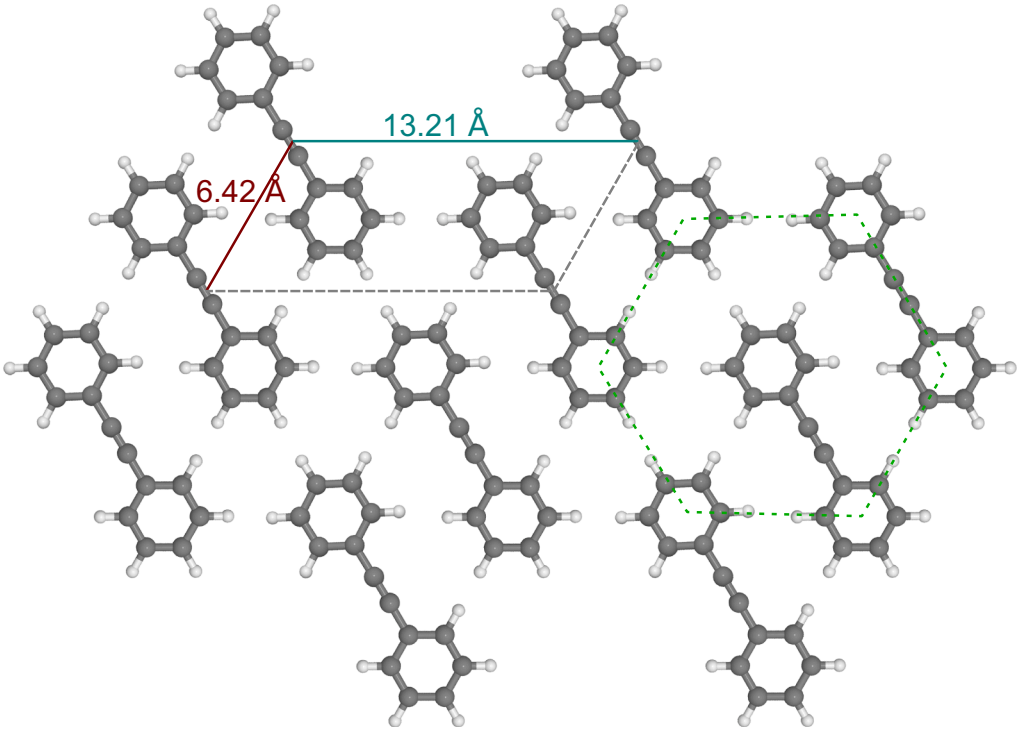

Fig. 5. Schematic, crystalline 2D arrangement of the nanothreads, represented by DPhA proxies, in the plane orthogonal to the thread axis. The monoclinic cell and the corresponding lattice parameters are evidenced as well as the hexagonal arrangement of the threads (dashed line). Grey and white spheres: C and H atoms, respectively.

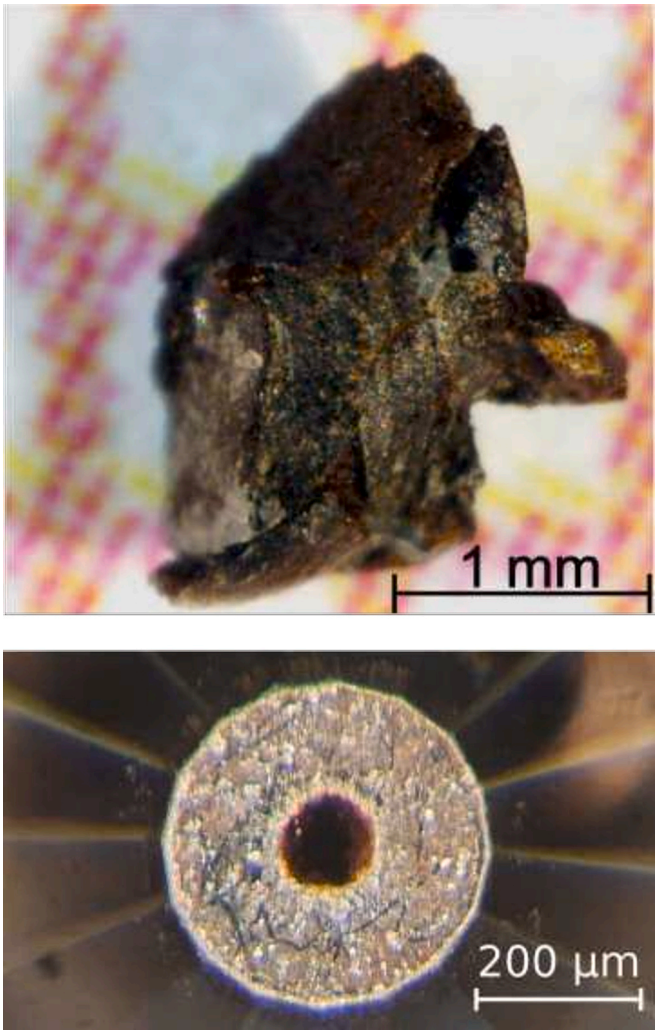

Fig. 6. Top panel: sample lump recovered after the MALVP synthesis. Bottom panel: sample recovered in DAC after a typical high pressure synthesis, shown in transmitted and reflected light.

linear size of the samples and of the X-ray beam spot for DACs was smaller than that of the MALVP/X-ray apparatus by 1–2 orders of magnitude, which in turn indicates that the compression of the MALVP sample was much more uniform than that of the DAC samples. Although we note that the reduced azimuth angular range of MALVP data could lead to slightly underestimating the actual pressure gradients. These findings go together with the pressure being applied much more isotropically in the MALVP, and all this immediately raises the question of how the difference between the two types of compression would affect the final synthesized materials.

The Bragg peaks of DPhA broaden and weaken substantially with increasing pressure, particularly above 15–16 GPa, which in fact corresponds to the reaction threshold for the formation of C-nanothreads observed in DACs [20]. A very faint peak observed in DACs at about 0.62 Å, above 9 GPa, and assigned to a potential new phase of molecular DPhA, which was supposed to be precursor of the nanothreads, was not observed here either due to the lower signal-to-noise ratio or because this phase was simply not present in the MALVP sample. In Fig. 3, we report the compression curves of the molecular DPhA crystal for the MALVP sample and for two DAC samples up to 16–17 GPa, in terms of V/V_0, where V and V_0 are the unit cell volumes at high and ambient pressure, respectively.

For the MALVP sample, volume data were obtained from a limited set of six Bragg peaks, marked by red dots in Fig. 2, which remain

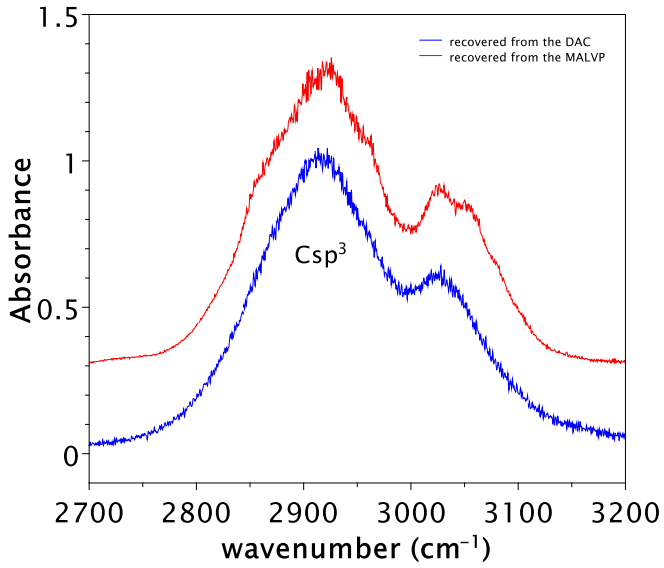

Fig. 7. IR absorption spectra of the MALVP (red) and the DAC (blue) recovered samples, both obtained after compression of diphenylacetylene to 30 GPa, in the frequency region of the C—H stretching modes. The most intense, broad peak centred at around 2920 cm^{-1} is the signature for carbon in sp^3, diamond-like hybridization forming the non-molecular material, whereas weaker peaks above 3000 cm^{-1} show the presence of some amount of residual highly strained, most likely amorphous molecular materials. To measure the spectrum of the MALVP sample, a small piece of material was taken from the main millimetric sample and pelleted into the gasket hole of a DAC to a final thickness of 25–30 μm. The two spectra have been vertically shifted for the sake of clarity. (For interpretation of the references to colour in this figure legend, the reader is referred to the web version of this article.)

sufficiently strong and resolved through the entire pressure range over which the compression curve is reported. Four out of six of these peaks are actually assigned to 2–3 distinct, yet poorly resolved d-spacings. We evaluated the compression curve by adopting two different procedures, here referred to as cc1 and cc2. As a first common step, we fitted a pseudo-Voigt function to each observed peak and obtained six distinct d-spacing values at each pressure. For cc1, we assigned the Miller indices to the d-spacings, according to the given known crystal structure at ambient pressure (monoclinic, $P2_1/c$). When more than one Bragg reflection was expected around a certain d-spacing, which could not be experimentally resolved, we assigned the observed reflection to the strongest expected one. We then analytically calculated the unit cell volumes. Instead, for cc2, we have not assumed any particular crystal structure and, as a consequence, we have not assigned Miller indices to the d-spacings. In this case, an effective compression curve was obtained as: $V/V_0 = (d/d_0)^3$, where the d-spacing ratio d/d_0 between the high and the ambient pressure values, respectively, has been averaged over the six peaks. The compression curves obtained through the two procedures, in fact, agree very well. We then fitted a Vinet equation of state function [25] through the MALVP cc1 data and obtained $B_0 = 12.7$ (3) GPa and $B_0' = 5.0$ (1), where B_0 and B_0' are the ambient pressure bulk modulus and its first derivative with respect to pressure, respectively. These values for the two parameters lie in the typical range of molecular crystals. Incidentally, we note that while our combined cc1/cc2 procedure may have underestimated possible high pressure phase transformations in the molecular DPhA, it has the advantage of clearly showing how smooth the compression curve of the molecular material is (see below for comparison to compressions in DAC) just up to the reaction threshold, which was one of the main purposes of our work.

The compression curves for the DAC samples also reported in Fig. 3 were obtained from the same set of data presented previously, where DPhA was compressed without PTM [20]. In this case, the unit cell

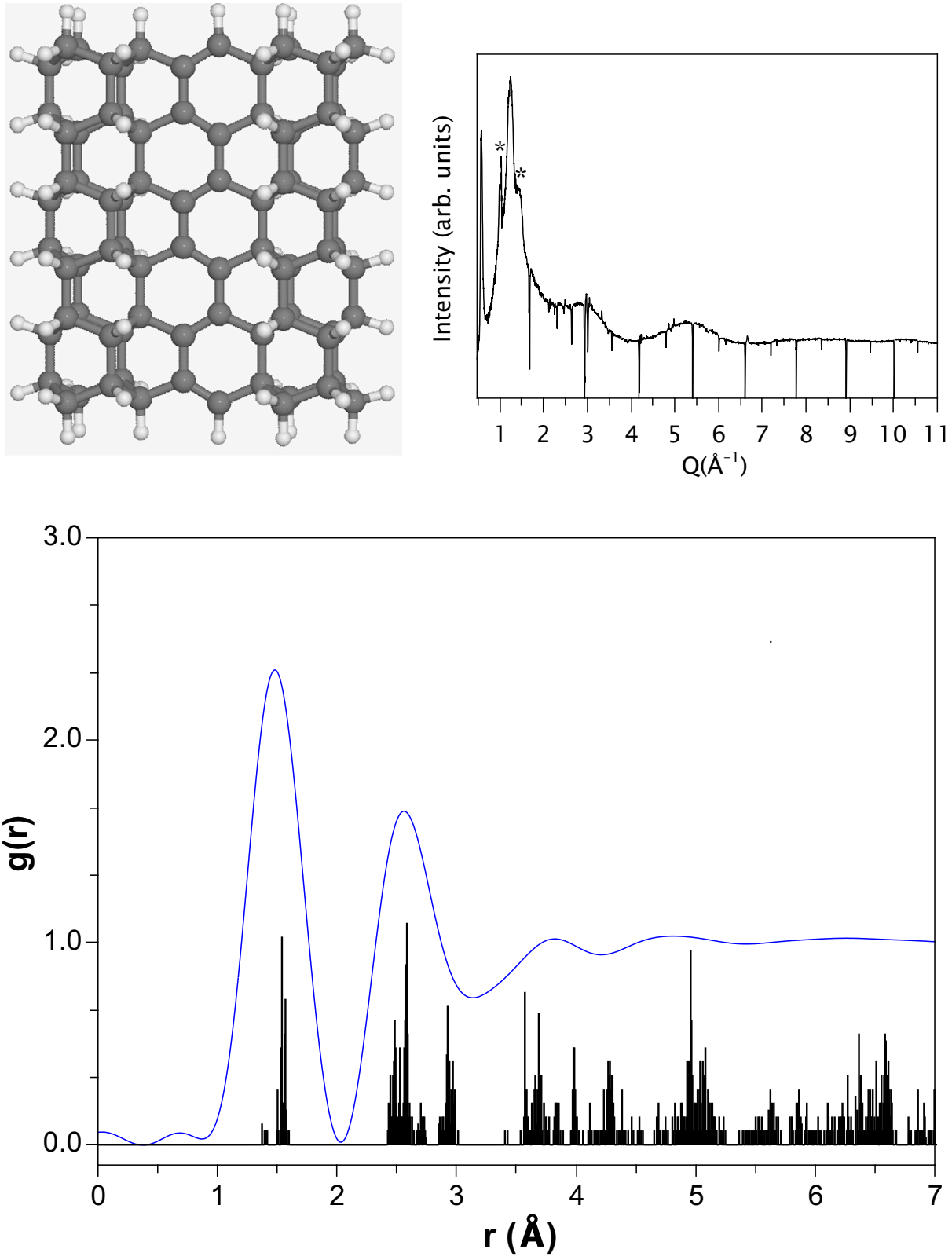

Fig. 8. Bottom panel: pair distribution function (blue line) of the post synthesis MALVP recovered sample, obtained from the total X-ray scattering pattern, using the Amorpheus software [26]. The numerical density ($\rho = 0.0875$ atoms/Å^3) was obtained as a combination of the present structural data and previous ab initio DFT computer simulations describing the internal structure of double-core nanothreads, named conjugated C-tube (3,0) [20]. This density value is about 30 % higher than that of the starting molecular crystal. Bottom panel, black pattern: statistical distribution for the interatomic CC distances in the DFT structural model of an isolated, double-core nanothread; here the amplitude has been rescaled for the sake of clarity. Top-left panel: DFT optimized structure of a nanothread fragment of the type: conjugated C-tube (3,0) [20]. Grey and white spheres: C and H atoms, respectively. Top-right panel: total X-ray scattering pattern of the MALVP recovered sample ($\lambda = 0.233933$ Å). Glitches are due to the gaps between the detector chips and asterisks indicate Bragg peaks from the supporting tape. (For interpretation of the references to colour in this figure legend, the reader is referred to the web version of this article.)

volumes were evaluated through a Le Bail fitting procedure of the measured XRD patterns. At variance with the MALVP compression curves, those obtained with DACs where largely not reproducible and one of the two curves also exhibits a sort of kink at around 5 GPa, together with an anomalous slope change and even a curvature change going from normal positive to slightly negative across the kink. These results clearly show that the DAC samples were compressed much less hydrostatically than the MALVP sample, as observed above from the direct observation of width of the Bragg peaks, likely due to the strong uniaxial stress present in the DACs.

It is now compelling to show how the greater hydrostaticity of the MALVP compression run affected the synthesized materials, which in fact is one of the main objectives of the present investigation. In Fig. 4, we report two XRD patterns measured on the free standing, post-synthesis recovered sample, which was extracted from the octahedral assembly and held on a tape through the X-ray beam. The two patterns were measured at two distinct points several hundred microns apart, with the X-ray spot size of about 1 mm^2, comparable to the sample size. Thus, the two patterns sampled two partially overlapping regions which, taken together, covered about the entire size of the recovered material. The broad and strong Compton background from the long (~2 m) sample-detector air path has been measured and subtracted. Clearly, the patterns are dominated by two sharp peaks located at 0.5835 (3) $Å^{-1}$ and 1.233 (3) $Å^{-1}$, respectively, indicating that a major portion of our samples is crystalline. On the other hand, the peak at higher Qs is build up on a more diffuse, significantly broader and weaker peak, which suggests the simultaneous presence of some amount of a highly disorder form in the sample, hence the composite nature of the material as a whole. The two-peak crystalline patterns are very similar to those observed for composite materials incorporating 1D DPhA-derived double-core carbon nanothreads obtained in DACs and also recovered at ambient pressure [20] (see Table 1). We then indexed the current patterns in a similar fashion and, consequently, identified our large-volume samples as consisting, to a substantial extent, of pseudo-hexagonal, monoclinic 2D packing of double-core nanothreads. More precisely, the freshly synthesized sample from the MALVP appears to be a slightly more packed version of this very peculiar structure, while we found it relaxed, over a period of about two weeks, to lower packing, more similar or slightly lower than to those of the DAC samples (see Table 1). Similar to the DAC samples, the peak width of the diffraction peaks leads us to estimate the transverse spatial correlation length for our nanothreads in a range, at least, between a few tens and about a hundred of Ångstrom. Following the interpretation given previously for DAC samples [20], we describe the present nanothread structure by means of a 2D monoclinic primitive cell (a = 6.42 Å, c = 13.21 Å, β = 120°, for the relaxed sample) reported in Fig. 5, where the 1D double-core nanothreads are represented by DPhA proxies. According to our previous study, based on a combination of XRD, infrared spectroscopy and density functional theory (DFT) simulations, these nanothreads are made of two diamond-like hydrogenated carbon-nanothreads, in fact the cores, linked by a conjugated backbone, which makes the material a low-bandgap polymer (E_{gap} = 1.74 eV for the rather brownish samples obtained in DACs). In agreement with these previous observations, the large volume sample recovered in this study is also a brownish material, hence a typically low-bandgap one (see Fig. 6 where we also report a typical recovered sample from the high pressure synthesis in DACs), while instead the initial DPhA solid is a transparent, colourless material.

In Fig. 7, we report IR absorption spectra of the MALVP and the DAC recovered samples, both obtained after compressions to 30 GPa, in the frequency region of the C—H stretching modes. The two spectra are entirely similar. The most intense, broad peak centred at around 2920 cm^{-1} is the signature for carbon in sp^3, diamond-like hybridization (Csp^3H groups) forming the non-molecular material; two very weak shoulders at 2860 cm^{-1} and 2960 cm^{-1}, respectively, in the MALVP sample, originate from defective Csp^3H_2 groups in this material. The weak peaks above 3000 cm^{-1} (Csp^2H groups) show the presence of some amount of residual highly strained, most likely amorphous molecular materials. These results are a direct evidence that the non-molecular recovered MALVP sample has the same local structure as the DAC sample, with respect to hydrogenated carbon, which in turn agrees with the carbon nano-thread structure described through the XRD investigation.

In Fig. 8, we also report the pair distribution function (PDF) for this sample. Needless to say, this function, as obtained by the XRD data, is substantially sensitive to the carbon-carbon correlation only. We observe two distinct well resolved peaks at 1.48 Å and 2.58 Å, deriving from the first (bonded atoms) and the second atomic coordination shells, respectively. The width of the two peaks is resolution limited. In the same figure, we also report the statistical distribution for the interatomic CC distances in the DFT structural model of an isolated, double-core nanothread, which we simulated previously and named conjugated C-tube (3,0) [20]. The agreement between the simulated CC distances and those observed experimentally is very good up to at least the fourth coordination shell, at around 5 Å, which in turn confirms the DFT structural model.

4. Conclusions

We synthesized a DPhA-derived polymeric composite material incorporating, to a substantial extent, carbon nanothreads by using a multi-anvil large volume press apparatus and performed materials characterization via synchrotron XRD and IR spectroscopy. The compression of the samples was quasi-isotropic, in contrast to those in DACs. Yet, the polymeric samples synthesized in MALVP and in DACs are fully comparable, on a quantitative basis. These results are direct evidence that the relevant reaction mechanisms are dominated by the favourable intrinsic relative orientation between nearest neighbour molecules in the initial molecular crystal, and it is very likely that this is extendable to similar aromatic systems such as azobenene and stilbene among others. In addition, the present synthesis method for carbon nanothreads provides the largest possible volume (a few mm^3) among those available for different high pressure cells: PE, DAC, at the reaction pressure of 30 GPa here in play, a result of potential practical interest for future applications of carbon nanothreads.

CRediT authorship contribution statement

S. Fanetti: sample preparation, XRD and IR measurements, data analysis and interpretation. **S. Romi**: sample preparation, XRD measurements, data analysis and interpretation. **W. Crichton**: sample preparation, XRD measurements, data analysis and interpretation. **A. Rosenthal**: sample preparation, XRD measurements. **D. Scelta**: sample preparation, XRD and IR measurements. **F. Alabarse**: sample preparation, XRD measurements. **R. Bini**: XRD and IR measurements, data interpretation. **M. Santoro**: project planning, sample preparation, XRD and IR measurements, data analysis and interpretation, conceptualization, and writing the manuscript.

All the authors have contributed to review the manuscript.

Declaration of competing interest

The authors declare that they have no known competing financial interests or personal relationships that could have appeared to influence the work reported in this paper.

Data availability

Data will be made available on request.

Acknowledgements

We acknowledge the European Synchrotron Radiation Facility and

Elettra-Sincrotrone Trieste for providing access to the ID06-LVP and Xpress beam-lines, respectively, and for financial support under the proposal numbers CH-6138 (ESRF) and 20200162 and 20205110 (Elettra). We also thank the Fondazione Cassa di Risparmio di Firenze for the strong support through the SALUS Grant.

References

[1] T.C. Fitzgibbons, M. Guthrie, E. Xu, V.H. Crespi, S.K. Davidowski, G.D. Cody, et al., Benzene-derived carbon nanothreads, Nat. Mater. 14 (2015) 43–47.
[2] B. Chen, R. Hoffmann, N.W. Ashcroft, J. Badding, E. Xu, V. Crespi, Linearly polymerized benzene arrays as intermediates, tracing pathways to carbon nanothreads, J. Am. Chem. Soc. 137 (2015) 14373–14386, https://doi.org/10.1021/jacs.5b09053.
[3] X. Li, M. Baldini, T. Wang, B. Chen, E.-S. Xu, B. Vermilyea, et al., Mechanochemical synthesis of carbon nanothread single crystals, J. Am. Chem. Soc. 139 (2017) 16343–16349, https://doi.org/10.1021/jacs.7b09311.
[4] A. Biswas, M.D. Ward, T. Wang, L. Zhu, H.-T. Huang, J.V. Badding, et al., Evidence for orientational order in nanothreads derived from thiophene, J. Phys. Chem. Lett. 10 (2019) 7164–7171, https://doi.org/10.1021/acs.jpclett.9b02546.
[5] D. Gao, X. Tang, J. Xu, X. Yang, P. Zhang, G. Che, Crystalline c3n3h3 tube (3,0) nanothreads, Proc. Natl. Acad. Sci. U. S. A. 119 (2022), e2201165119, https://doi.org/10.1073/pnas.2201165119.
[6] S.G. Dunning, L. Zhu, B. Chen, S. Chariton, V.B. Prakapenka, M. Somayazulu, T. A. Strobel, Solid-state pathway control via reaction-directing heteroatoms: ordered pyridazine nanothreads through selective cycloaddition, J. Am. Chem. Soc. 144 (2022) 2073–2078, https://doi.org/10.1021/jacs.1c12143.
[7] X. Li, T. Wang, P. Duan, M. Baldini, H.-T. Huang, B. Chen, et al., Carbon nitride nanothread crystals derived from pyridine, J. Am. Chem. Soc. 140 (2018) 4969–4972, https://doi.org/10.1021/jacs.7b13247.
[8] S. Fanetti, M. Santoro, F. Alabarse, B. Enrico, R. Bini, Modulating the h-bond strength by varying the temperature for the high pressure synthesis of nitrogen rich carbon nanothreads, Nanoscale 12 (2020) 5233–5242.
[9] S. Huss, S. Wu, B. Chen, T. Wang, M.C. Gerthoffer, D.J. Ryan, et al., Scalable synthesis of crystalline one-dimensional carbon nanothreads through modest-pressure polymerization of furan, ACS Nano 15 (2021) 4134–4143, https://doi.org/10.1021/acsnano.0c10400.
[10] B. Matsuura, S. Huss, Z. Zheng, S. Yuan, T. Wang, B. Chen, et al., Perfect and defective13c-furan-derived nanothreads from modest-pressure synthesis analyzed by 13c nmr, J. Am. Chem. Soc. 143 (2021) 9529–9542, https://doi.org/10.1021/jacs.1c03671.
[11] M.M. Nobrega, E. Teixeira-Neto, A.B. Cairns, M.L.A. Temperini, R. Bini, One-dimensional diamondoid polyaniline-like nanothreads from compressed crystal aniline, Chem. Sci. 9 (2018) 254–260.
[12] S. Fanetti, M.M. Nobrega, E. Teixeira-Neto, M.L.A. Temperini, R. Bini, Effect of structural anisotropy in high-pressure reaction of aniline, J. Phys. Chem. C 122 (2018) 29158–29164.
[13] M.C. Gerthoffer, S. Wu, B. Chen, T. Wang, S. Huss, S.M. Oburn, et al., 'sacrificial' supramolecular assembly and pressure-induced polymerization: toward sequence-defined functionalized nanothreads, Chem. Sci. 11 (2020) 11419–11424, https://doi.org/10.1039/D0SC03904G.
[14] W.S. Tang, T.A. Strobel, Evidence for functionalized carbon nanothreads from π-stacked, Para-disubstituted benzenes, J. Phys. Chem. C 124 (2020) 25062–25070, https://doi.org/10.1021/acs.jpcc.0c06715.
[15] S. Romi, S. Fanetti, F. Alabarse, A.M. Mio, R. Bini, Synthesis of double core chromophore-functionalized nanothreads by compressing azobenzene in a diamond anvil cell, Chem. Sci. 12 (2021) 7048–7057.
[16] S. Romi, S. Fanetti, F. Alabarse, R. Bini, Structure-reactivity relationship in the high-pressure formation of double-core carbon nanothreads from azobenzene crystal, J. Phys. Chem. C 125 (2021) 17174–17182, https://doi.org/10.1021/acs.jpcc.1c04003.
[17] S. Romi, S. Fanetti, R. Bini, S. Fanetti, R. Bini, R. Bini, Towards custom built double core carbon nanothreads using stilbene and pseudo-stilbene type systems, Nanoscale 14 (2022) 4614–4625, https://doi.org/10.1039/d1nr08188h.
[18] M.D. Ward, W.S. Tang, L. Zhu, D. Popov, G.D. Cody, T.A. Strobel, Controlled single-crystalline polymerization of C10H8 • C10F8 under pressure, Macromolecules 52 (2019) 7557–7563, https://doi.org/10.1021/acs.macromol.9b01416.
[19] A. Friedrich, I.E. Collings, K.F. Dziubek, S. Fanetti, K. Radacki, J. Ruiz-Fuertes, et al., Pressure-induced polymerization of polycyclic arene-perfluoroarene cocrystals: single crystal x-ray diffraction studies, reaction kinetics, and design of columnar hydrofluorocarbons, J. Am. Chem. Soc. 142 (2020) 18907–18923.
[20] S. Romi, S. Fanetti, F. Alabarse, R. Bini, M. Santoro, High pressure synthesis of 1D low-bandgap polymers embedded in diamond-like carbon nanothreads, Chem. Mater. 34 (2022) 2422–2428, https://doi.org/10.1021/acs.chemmater.1c04453.
[21] Y. Le Godec, D. Martinez-Garcia, M. Mezouar, G. Syfosse, J.-P. Itié, J.-M. Besson, Thermoelastic behaviour of hexagonal graphite-like boron nitride, High Pressure Res. 17 (2000) 35–46, https://doi.org/10.1080/08957950008200304.
[22] V. Solozhenko, D. Häusermann, M. Mezouar, M. Kunz, Equation of state of wurtzitic boron nitride to 66 GPa, Appl. Phys. Lett. 72 (1998) 1691–1693, https://doi.org/10.1063/1.121186.
[23] A. Hammersley, S. Svensson, M. Hanfland, A. Fitch, D. Häusermann, Two dimensional detector software: from real detector to idealised image or two-theta scan, High Pressure Res. 14 (1996) 235–248.
[24] R. Bini, R. Ballerini, G. Pratesi, H.J. Jodl, Experimental setup for fourier transform infrared spectroscopy studies in condensed matter at high pressure and low temperatures, Rev. Sci. Instrum. 68 (1997) 3154–3160.
[25] P. Vinet, J. Ferrante, J.R. Smith, J.H. Rose, A universal equation of state for solids, J. Phys. C Solid State Phys. 19 (1986) L467–L473, https://doi.org/10.1088/0022-3719/19/20/001.
[26] S. Boccato, Y. Garino, G. Morard, B. Zhao, F. Xu, C. Sanloup, et al., Amorpheus: a python-based software for the treatment of x-ray scattering data of amorphous and liquid systems, High Pressure Res. 42 (2022) 69–93, https://doi.org/10.1080/08957959.2022.2032032.